Stars and Dark Matter at the Center of the Milky Way

5th IDPASC PhD Student Workshop

José Lopes

supervised by **Prof. Ilídio Lopes**

co-supervised by **Prof. Joseph Silk**

Introduction

Evidence to Particle Dark Matter

Stars as Dark Matter Laboratories

Energy transport by Particle Dark Matter

The code: dmEFT

Results

Asteroseismology of Red Clump Stars with Dark Matter

(**Lopes**, Lopes & Silk, *submitted*)

ADM in the Nuclear Star Cluster: Low Mass Main-Sequence Stars

(**Lopes** & Lopes, *ApJ, in press*)

Conclusion

Summary

Introduction

Evidence to Particle Dark Matter

Stars as Dark Matter Laboratories

Energy transport by Particle Dark Matter

The code: dmEFT

Results

Asteroseismology of Red Clump Stars with Dark Matter

(**Lopes**, Lopes & Silk, *submitted*)

ADM in the Nuclear Star Cluster: Low Mass Main-Sequence Stars

(**Lopes** & Lopes, *ApJ, in press*)

Conclusion

Summary

Evidence to particle dark matter

Galaxy rotation curves, Bullet cluster, gravitational lensing, etc. (e.g., **Zwicky 1933; Rubin et al. 1970; Tucker et al. 1998**).

Λ-Cold Dark Matter Cosmology and CMB anisotropies.

Particle Physics models could resolve other major problems (Supersymmetry, axions, etc.).

X-ray: NASA/CXC/CfA/ M.Markevitch et al.;
Lensing Map: NASA/STScI; ESO WFI; Magellan/U.Arizona/ D.Clowe et al.
Optical: NASA/STScI; Magellan/U.Arizona/D.Clowe et al.;

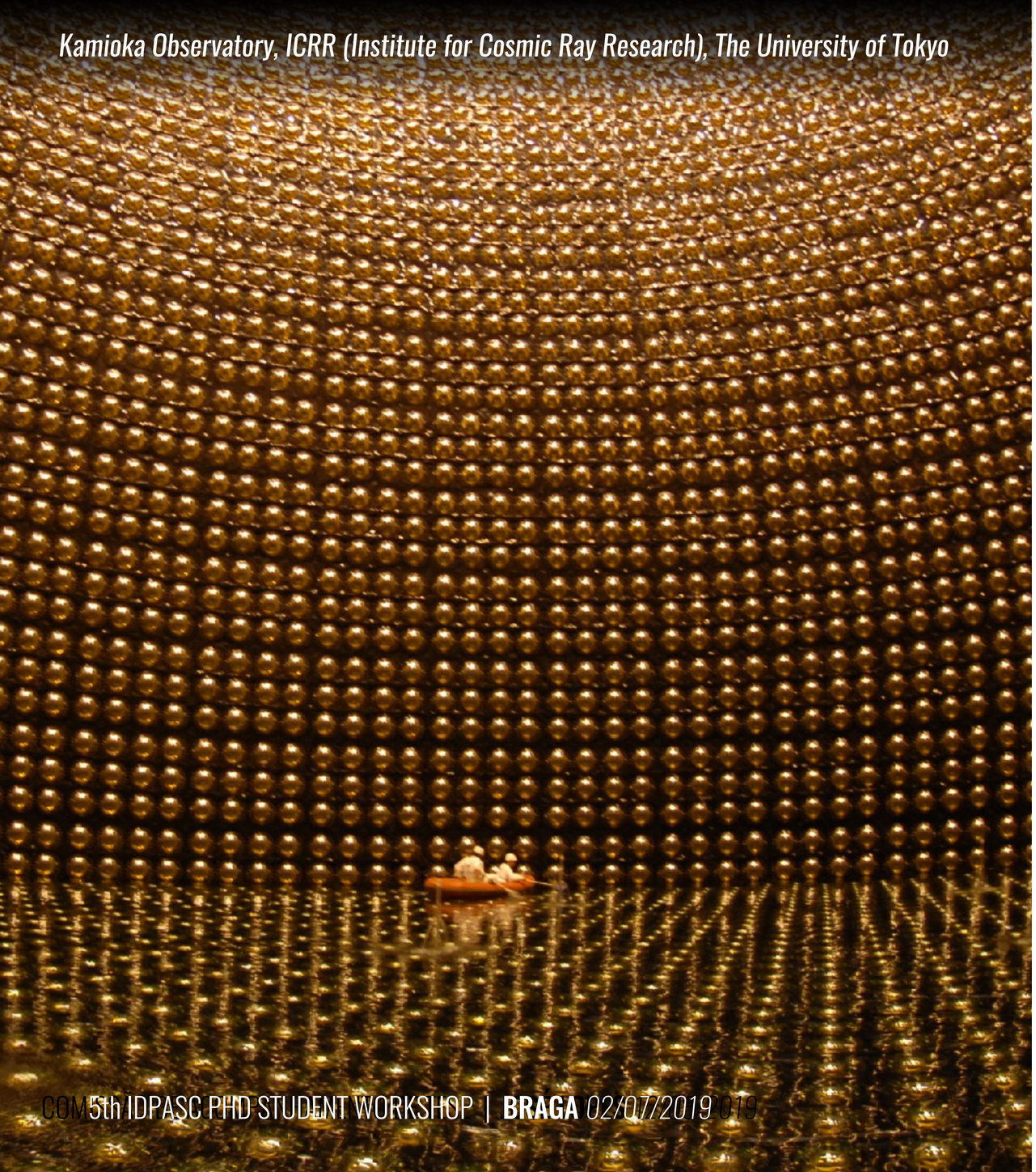
Kamioka Observatory, ICRR (Institute for Cosmic Ray Research), The University of Tokyo

Stars as dark matter laboratories

Detectors with huge effective volume and unique conditions.

Detect by-products of DM annihilation, such as, GeV neutrinos from de the Sun (e.g., **Choi et al. 2015**).

Search for manifestations or signatures of dark matter interactions within the stars - asteroseismology, photometry, stellar populations, etc. (e.g., **Spergel & Press 1985**; **Lopes & Silk 2002**; **Moskalenko & Wai 2007**).

Energy transport by particle dark matter

DM particles in the halo can get gravitationally captured inside a star (**Gould 1987**):

$$C_\odot = \sum_i \int_\odot \frac{\mathrm{d}C_{\odot,i}}{\mathrm{d}V}\mathrm{d}^3 r \qquad (1)$$

$$\frac{\mathrm{d}C_{\odot,i}}{\mathrm{d}V} = \int_0^\infty \mathrm{d}u \frac{f(u)}{u} w \Omega^-_{v_{e,i}}(w,r) \qquad (2)$$

$$\Omega^-_{v_{e,i}}(w,r) \propto \int \mathrm{d}E \frac{\mathrm{d}\sigma_{\chi,N_i}}{\mathrm{d}E}(w^2,q^2) \qquad (3)$$

Interactions with baryons in the stellar plasma provide an **additional energy transport mechanism** (**Spergel & Press 1985**):

$$\frac{\partial \ell}{\partial m} = \varepsilon_{\mathrm{nuc}} + \varepsilon_{\mathrm{neu}} - T\frac{\partial S}{\partial t} + \varepsilon_\chi \qquad (4)$$

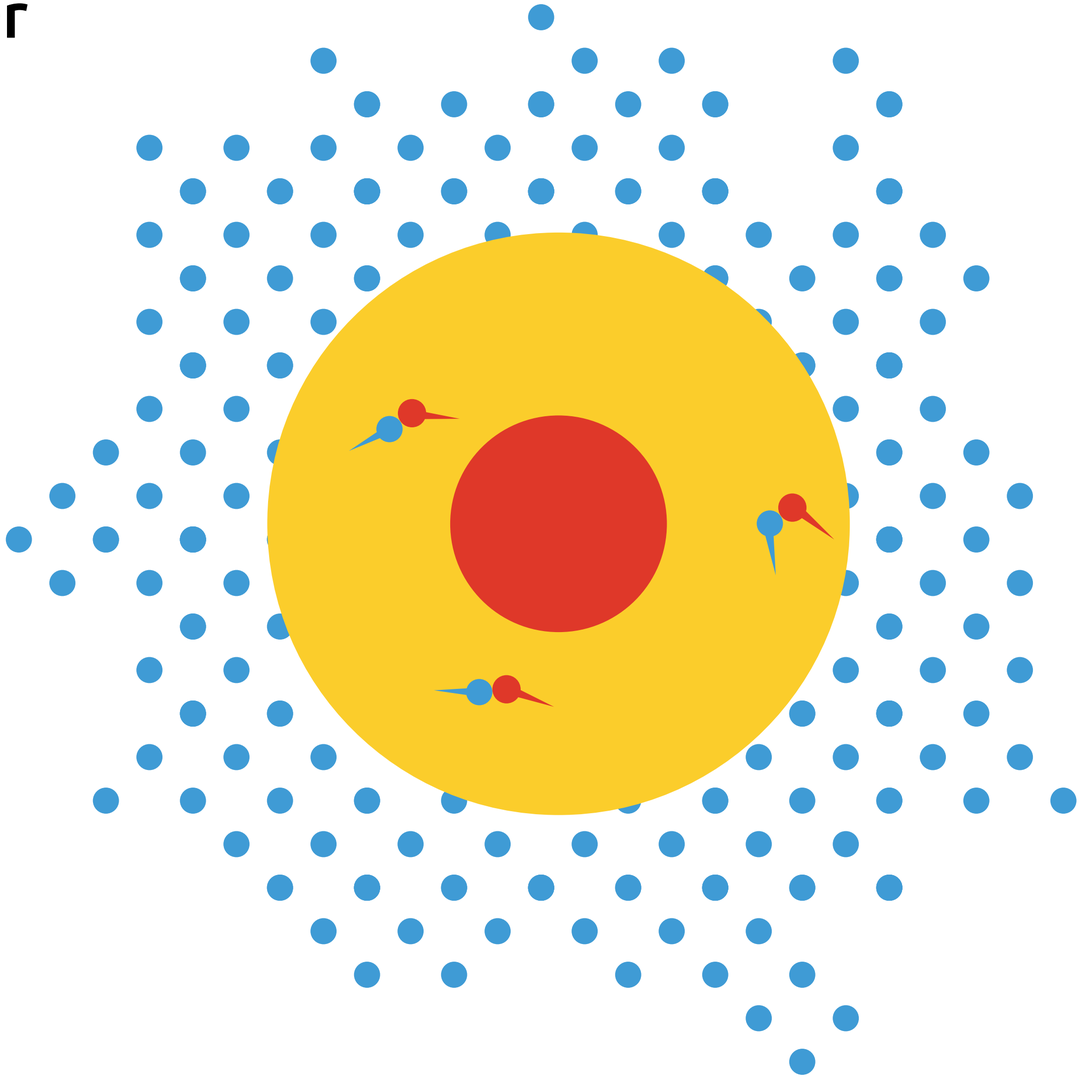

Energy transport by particle dark matter

DM particles in the halo can get gravitationally captured inside a star (**Gould 1987**):

$$C_\odot = \sum_i \int_\odot \frac{\mathrm{d}C_{\odot,i}}{\mathrm{d}V}\mathrm{d}^3 r \qquad (1)$$

$$\frac{\mathrm{d}C_{\odot,i}}{\mathrm{d}V} = \int_0^\infty \mathrm{d}u \frac{f(u)}{u} w\Omega^-_{v_{e,i}}(w,r) \qquad (2)$$

$$\Omega^-_{v_{e,i}}(w,r) \propto \int \mathrm{d}E \frac{\mathrm{d}\sigma_{\chi,N_i}}{\mathrm{d}E}(w^2,q^2) \qquad (3)$$

Interactions with baryons in the stellar plasma provide an **additional energy transport mechanism** (**Spergel & Press 1985**):

$$\frac{\partial \ell}{\partial m} = \varepsilon_{\mathrm{nuc}} + \varepsilon_{\mathrm{neu}} - T\frac{\partial S}{\partial t} + \varepsilon_\chi \qquad (4)$$

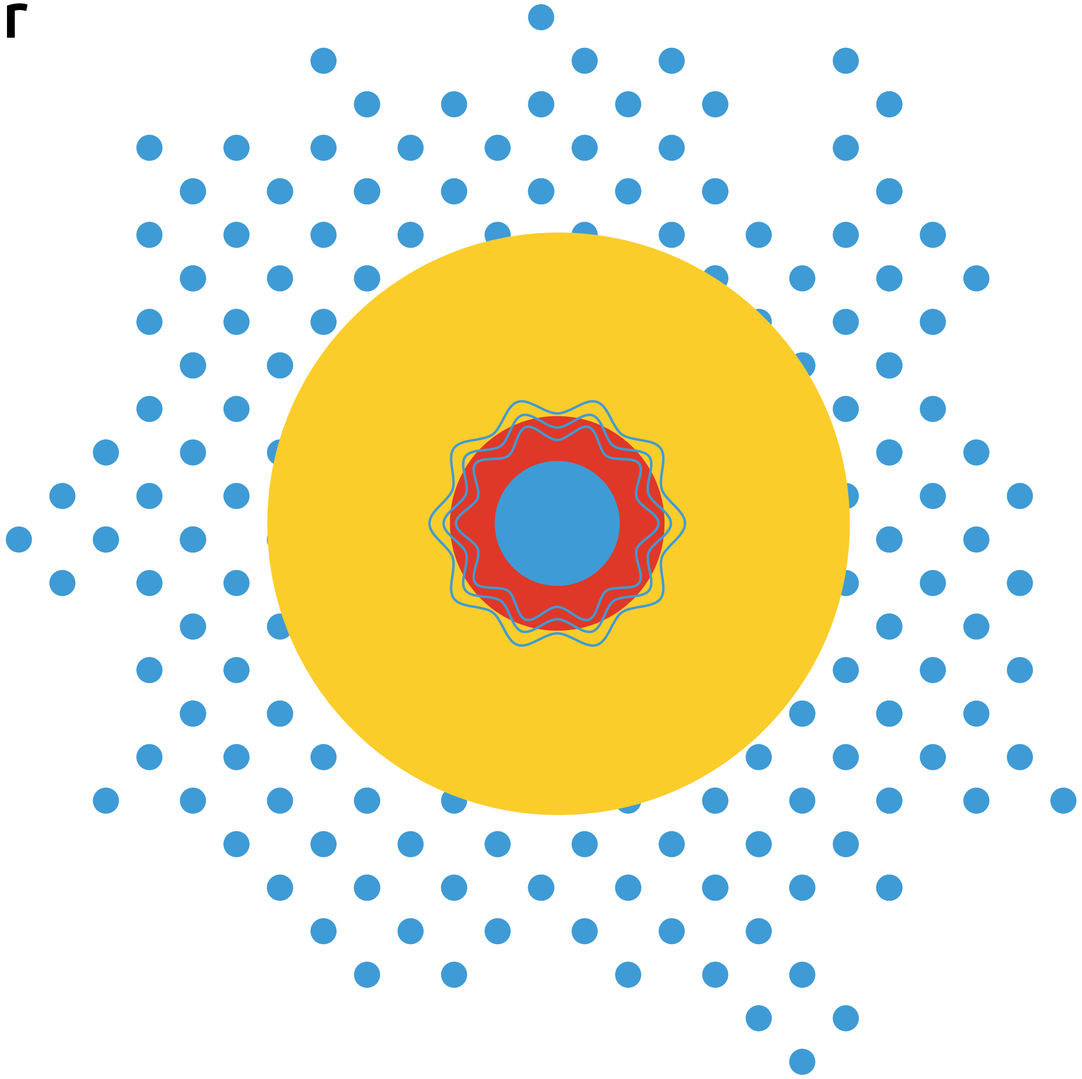

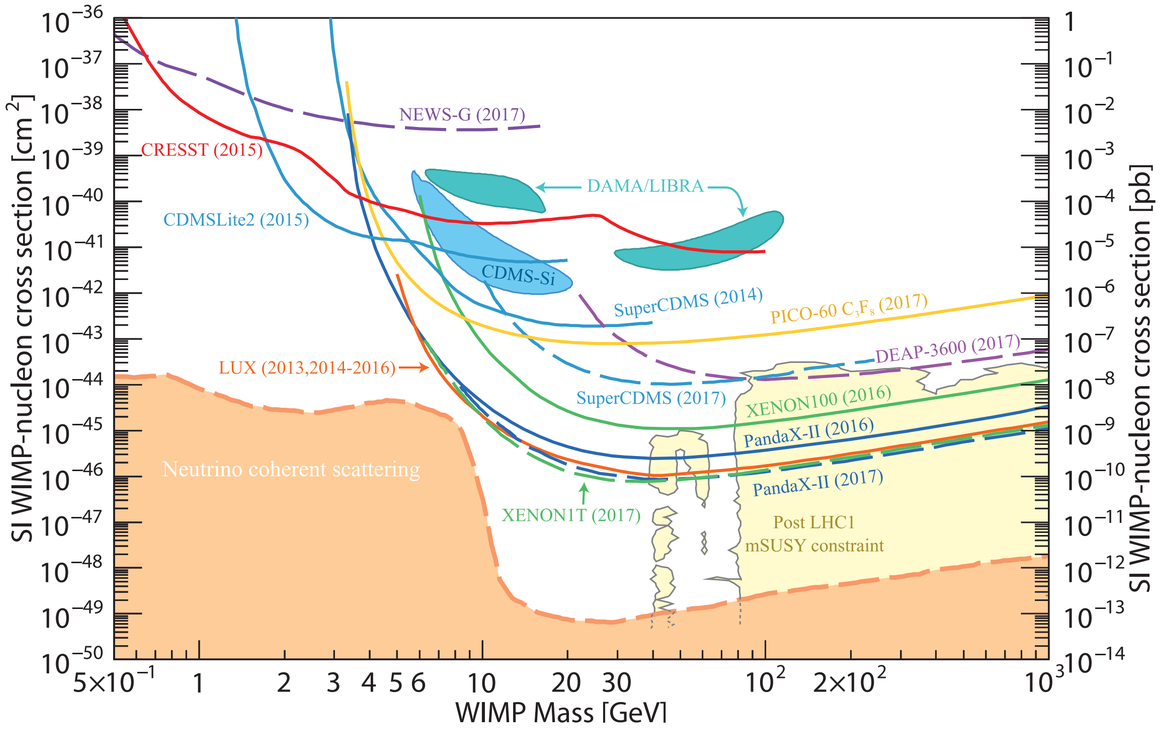

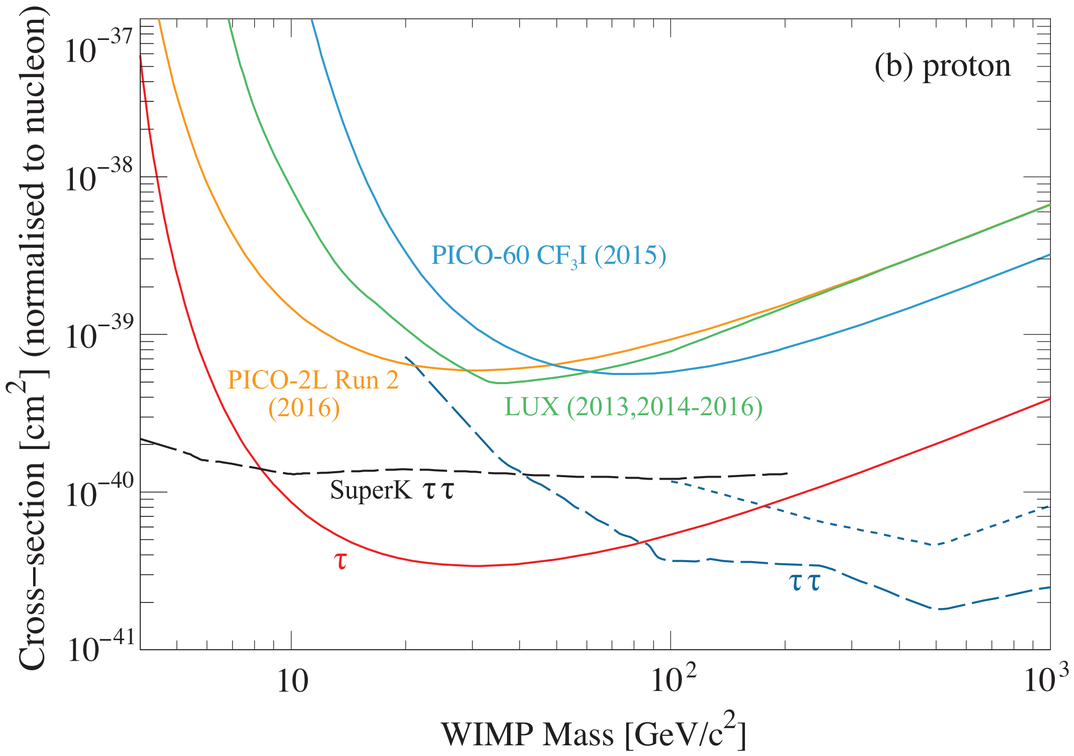

ANNEX II Left: Current constrains on the Dark Matter Spin Independent interaction cross-section ; **Right**: Current constrains on the Dark Matter Spin Dependent interaction cross-sectio (hydrogenn only). Adapted from **Tanabashi et al. (2018) (PDG).**

The code: dmEFT

dmEFT is built upon the widely used **MESA** stellar evolution code, in constant development and with ~1000 active users (**Paxton et al. 2011; 2013; 2015; 2018**).

Computes the dark matter phenomenology and models **robustly** (implicitly or explicitly) its **impact** in the evolution of the Star

Implemented with **modularity**, parallelized (*OpenMP*), with speed optimization.

First extension to MESA including a full description of Dark Matter (WIMP) framework.

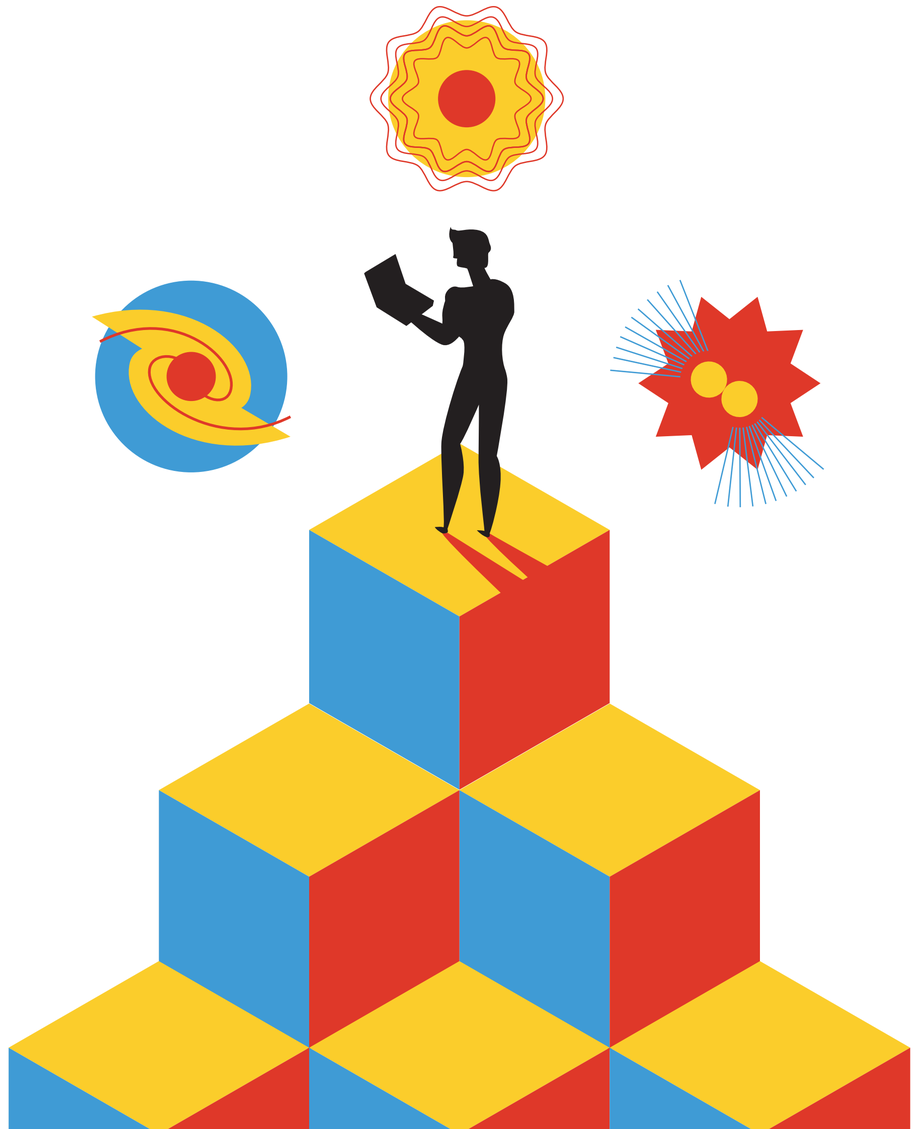

Introduction

Evidence to Particle Dark Matter

Stars as Dark Matter Laboratories

Energy transport by Particle Dark Matter

The code: dmEFT

Results

Asteroseismology of Red Clump Stars with Dark Matter

(**Lopes**, Lopes & Silk, *submitted*)

ADM in the Nuclear Star Cluster: Low Mass Main-Sequence Stars

(**Lopes** & Lopes, *ApJ, in press*)

Conclusion

Summary

Red Clump Stars: probes to dark matter

Low-mass core-helium-burning (CHeB) stars defining a sharp **clump** feature in the HR diagram;

Expected to constitute **31%** of all nearby giants, observed throughout the Milky way (L~100 L⊙),(**Girardi et al. 2009**);

Ideal to probe the dark matter density in the **galactic center** (r ~ 1 - 5 pc; $\rho_{DM} = 10^6 \rho_{DM,\odot}$);

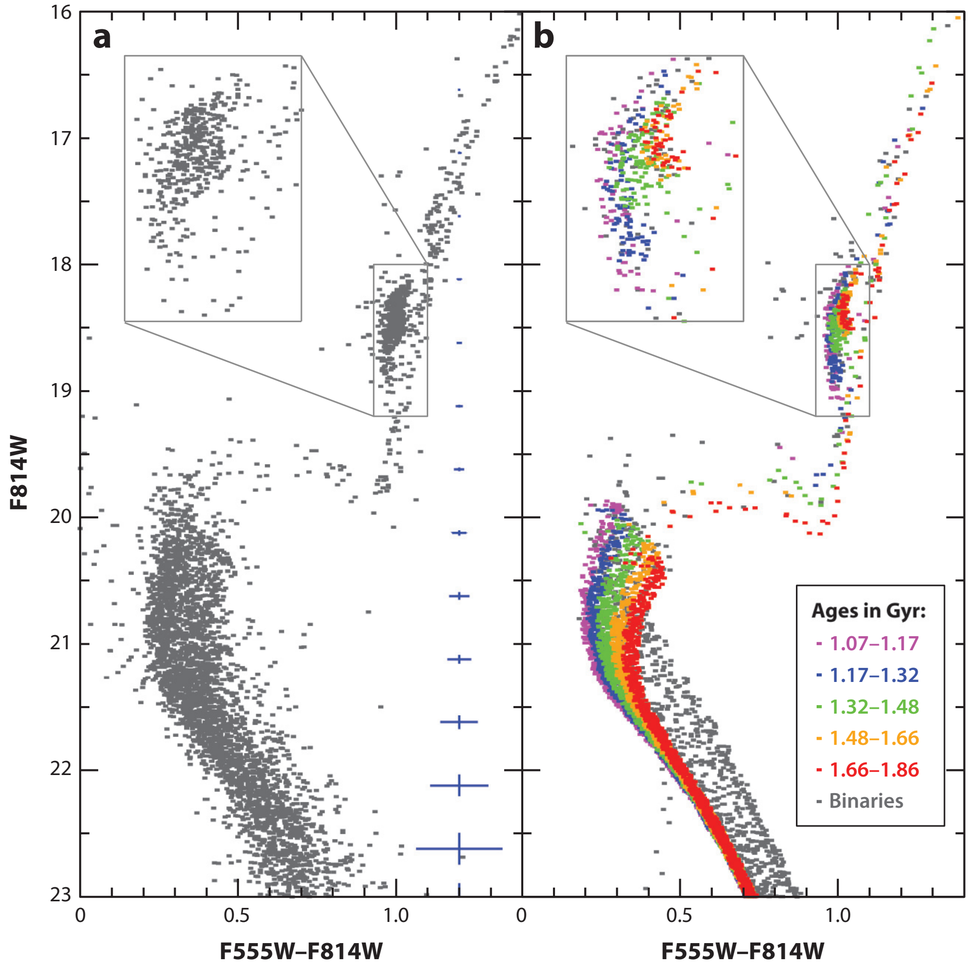

FIG. I *Hubble Space Telescope* Color-magnitude-diagram (CMD) for the **Pequena Nuvem de Magalhães** NGC 419 **(Girardi et al. 2009);**

Convective core suppression

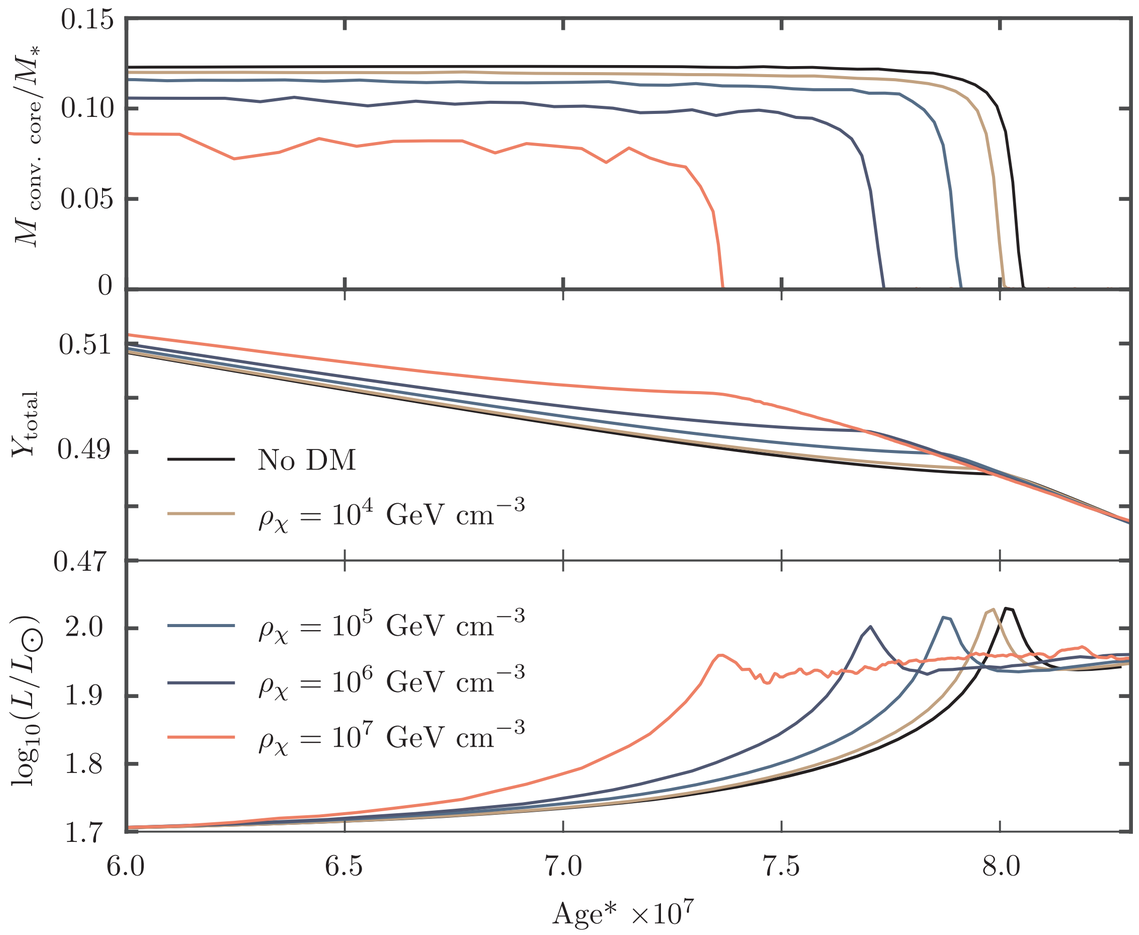

Dark Matter particles (m =4 GeV) **carry energy** away from nuclear burning regions;

Energy transport by dark matter particles **suppresses convection** in the stellar core (convective core up to **~30%** smaller);

Suppression of convection **quenches** the helium supply and ends the CHeB stage.

FIG. II Mass of the convective core, total helium content and total luminosity of a CHeB star with M = 1.0M$_\odot$ for different densities of dark matter (m = 4 GeV).

Asteroseismology of Red Clump Stars

Stars oscillate due to turbulent perturbations restored by pressure (**p-modes**) and buoyancy forces (**g-modes**).

The frequency of the oscillation modes can be used to probe the **interior** of the star (**Tassoul 1980**):

$$\Delta\nu = \left(2\int_0^R \frac{\mathrm{d}r}{c_s}\right)^{-1} \tag{5}$$

$$\Delta\Pi = \frac{2\pi^2}{\sqrt{l(l+1)}}\left(\int_{r_1}^{r_2} N\frac{\mathrm{d}r}{r}\right)^{-1} \tag{6}$$

Red Clump stars exhibit **mixed modes**, i.e., with p- and g-mode properties.

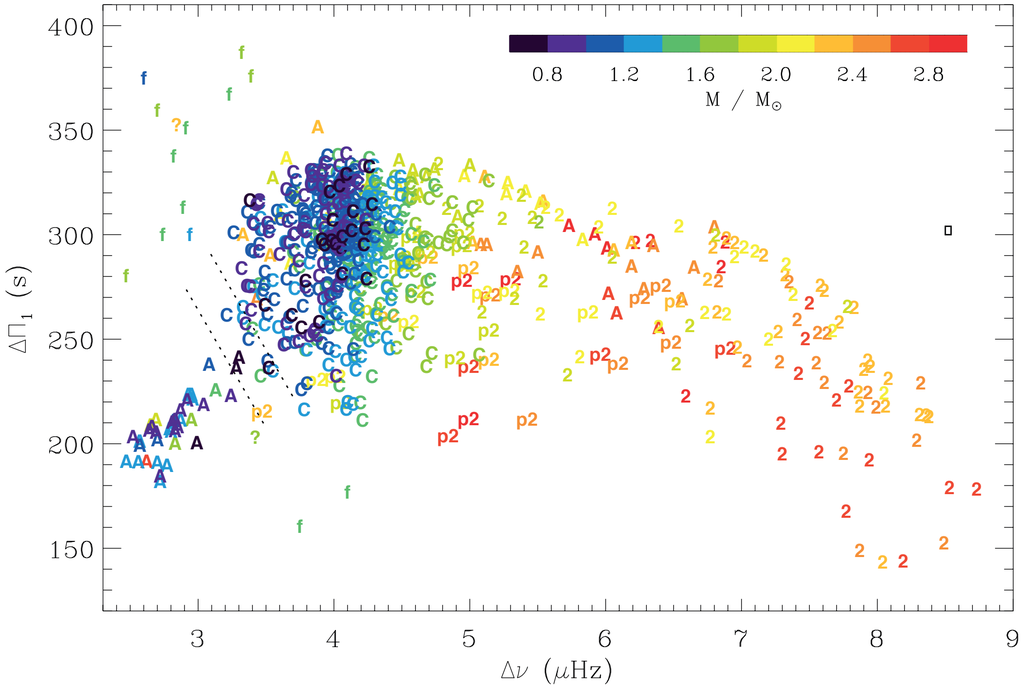

FIG. III Asteroseismic diagram for a set of stars chosen from the *Kepler* data including 541 Red Clump (**C**) stars exhibiting mixed modes **(Mosser et al. 2014).**

Asteroseis

Stars oscillat
restored by
forces (**g-moc**

The frequenc
used to prob
1980):

ΔI

Red Clump st
p- and g-mode

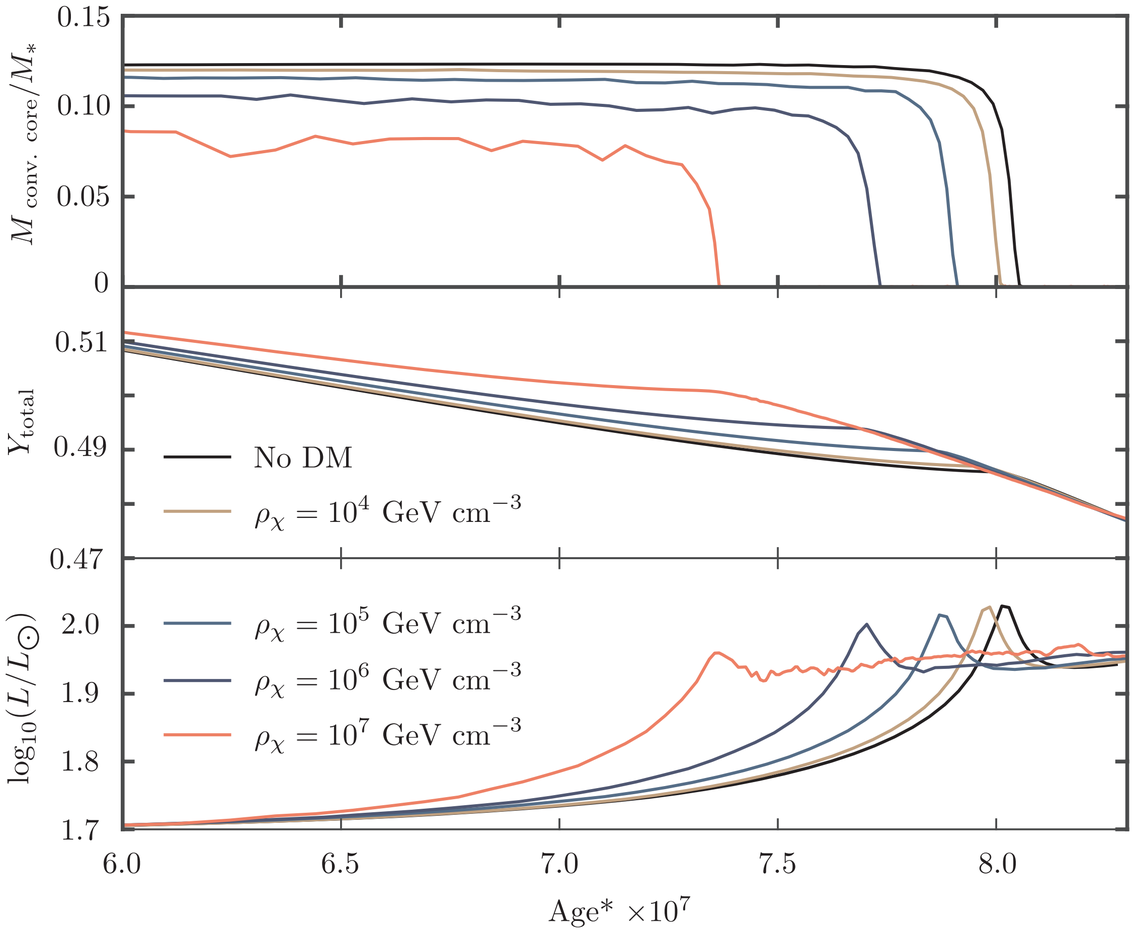

FIG. II Mass of the convective core, total helium content and total luminosity of a CHeB star with M = 1.0M$_\odot$ for different densities of dark matter (m = 4 GeV).

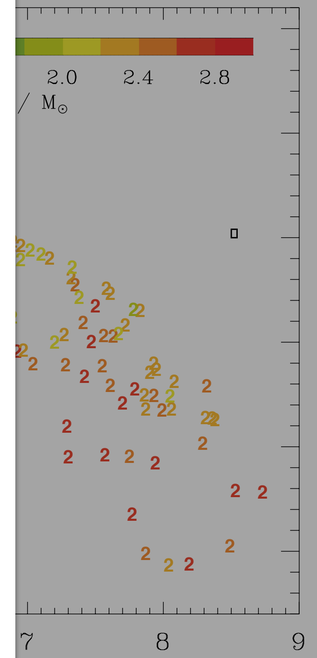

of stars chosen
Clump (**C**) stars
.

Dark Matter signature in the *large period separation*

Gravity oscillation modes, i.e., **g-modes**, are suppressed within convective regions;

The **large period separation** is related to the size of the convective core (**Montalbán et al. 2013**);

$$\Delta\Pi = \frac{2\pi^2}{\sqrt{l(l+1)}} \left(\int_{r_1}^{r_2} N \frac{\mathrm{d}r}{r} \right)^{-1} \qquad (6)$$

ΔΠ₁ can reflect a dark matter signature within the **precision** of current telescopes, represented by the white contours.

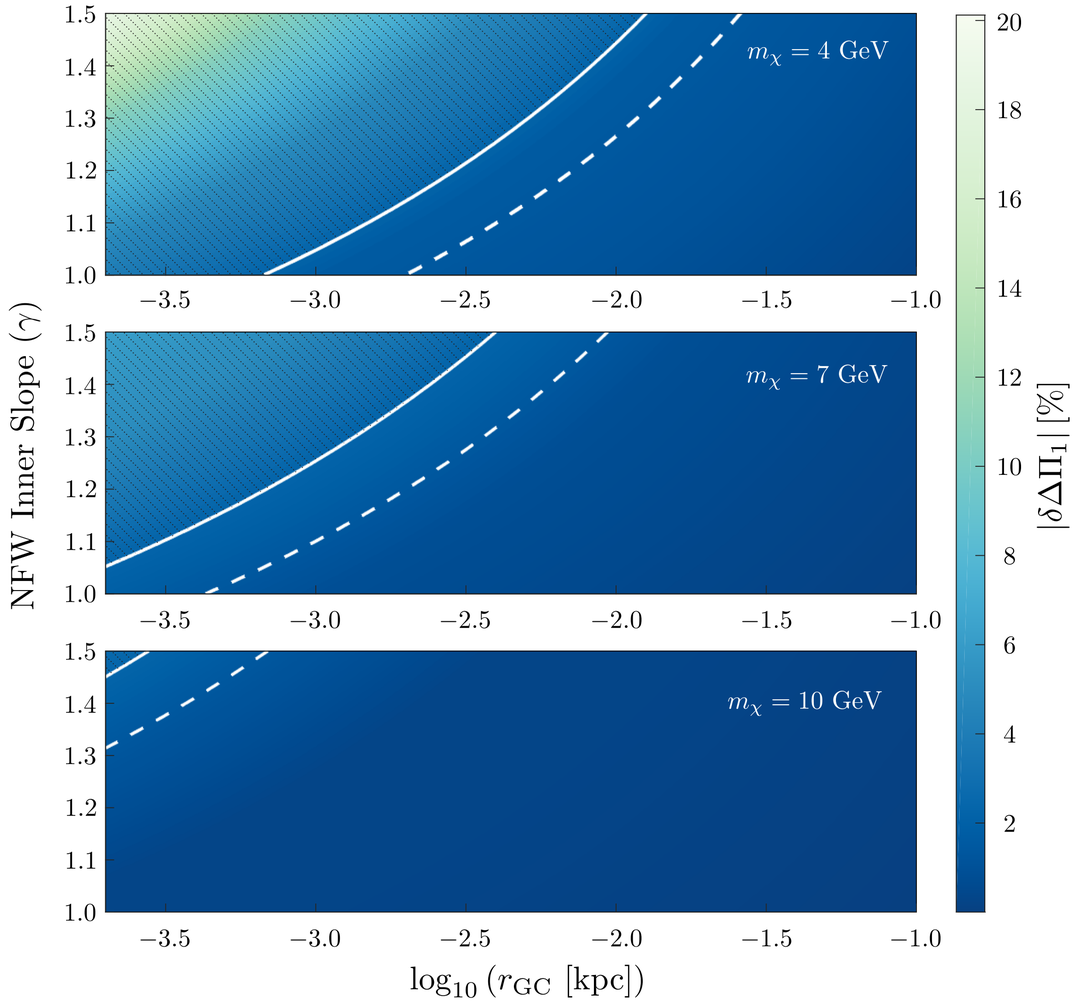

FIG. IV The deviation of the g-mode period separation **ΔΠ₁** as a function of the distance to the center of the galaxy.

Introduction

Evidence to Particle Dark Matter

Stars as Dark Matter Laboratories

Energy transport by Particle Dark Matter

The code: dmEFT

Results

Asteroseismology of Red Clump Stars with Dark Matter

(**Lopes**, Lopes & Silk, *submitted*)

ADM in the Nuclear Star Cluster: Low Mass Main-Sequence Stars

(**Lopes** & Lopes, *ApJ, in press*)

Conclusion

Summary

ADM in the nuclear star cluster: low mass main-sequence Stars

Asymmetric Dark Matter does not self-annihilate (**Kaplan et al. 2019**),

$$\frac{\mathrm{d}N_\chi}{\mathrm{d}t} \simeq C_\odot - \cancel{A_\odot} N_\chi^2 \qquad (7)$$

The Dark Matter density in the **Nuclear Star Cluster** of the Milky Way (half-light radius ~5 pc) is orders of magnitude above the local density.

Low-mass main-sequence stars are **sensitive** to DM coupling with **hydrogen** (difficult in direct detection).

Future (~10 years) 30-40 m class telescopes will **resolve** low-mass main sequence stars in the NGC.

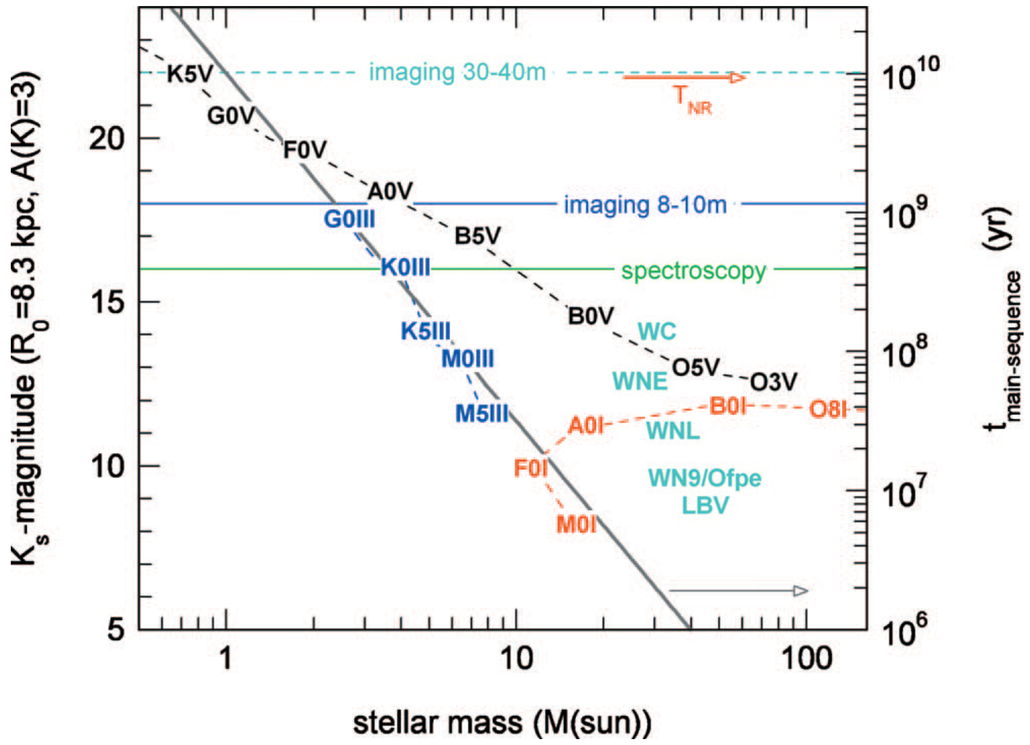

FIG. V Sensitivity of current and future telescopes in the Milky Way´s NSC. Main-sequence stars are identified by the spectral type **V**. From **Genzel et al. (2010).**

Effect 1: Hydrogen burning rate slowdown

ADM interactions with baryons will **decrease the temperature in the stellar core** (~10-20% lower temperature in a MS solar-mass star).

The cooling will **slow down the hydrogen nuclear burning rate** in stars with radiative core (M<1.2M⊙).

Stars will **spend more time** in the Main-Sequence (~30% longer). Low mass stars will have MS lifetime **comparable** to the Universe´s age.

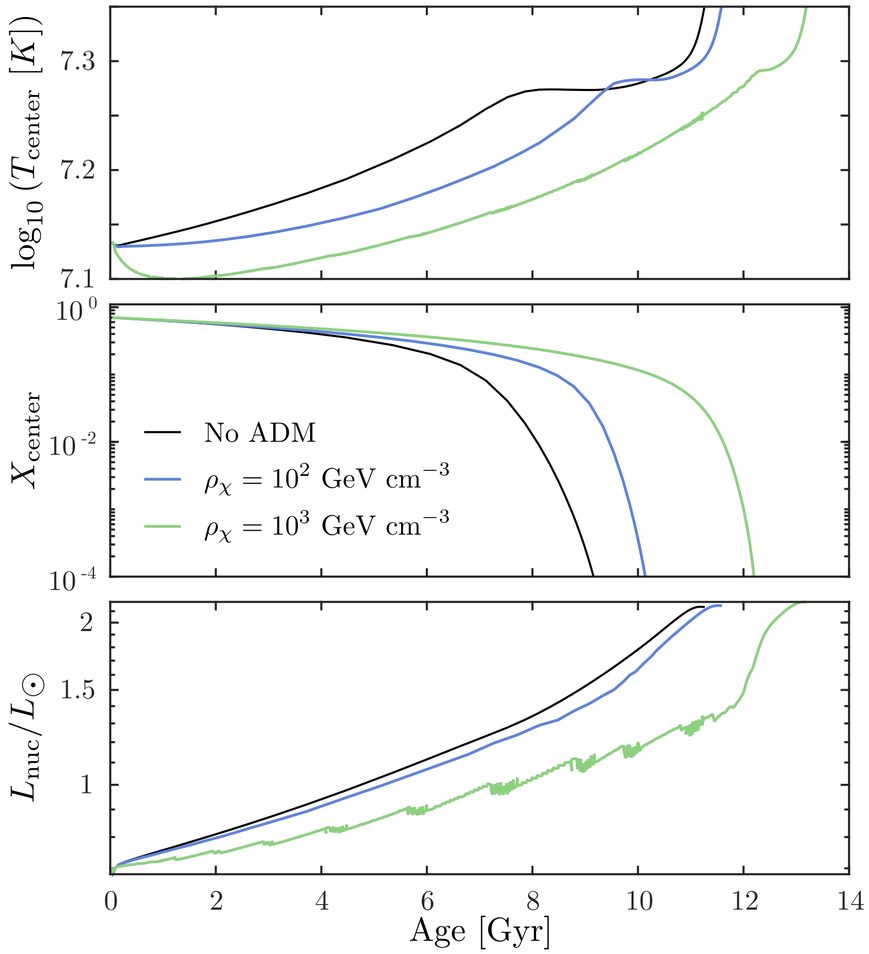

FIG. VI Evolution (central temperature, hydrogen and total nuclear luminosity) of a solar mass star in different ADM density scenarios

Effect 2: Convective core suppression

In stars with M>1.2M⊙ the core is too opaque for the energy produced in the CNO reactions -> **core convection**.

ADM particles can help evacuate the energy, **suppressing** core convection (for stars up to M~1.4M⊙).

Stars with core convection suppression will have **shorter** MS lifetimes due to the quench of hydrogen.

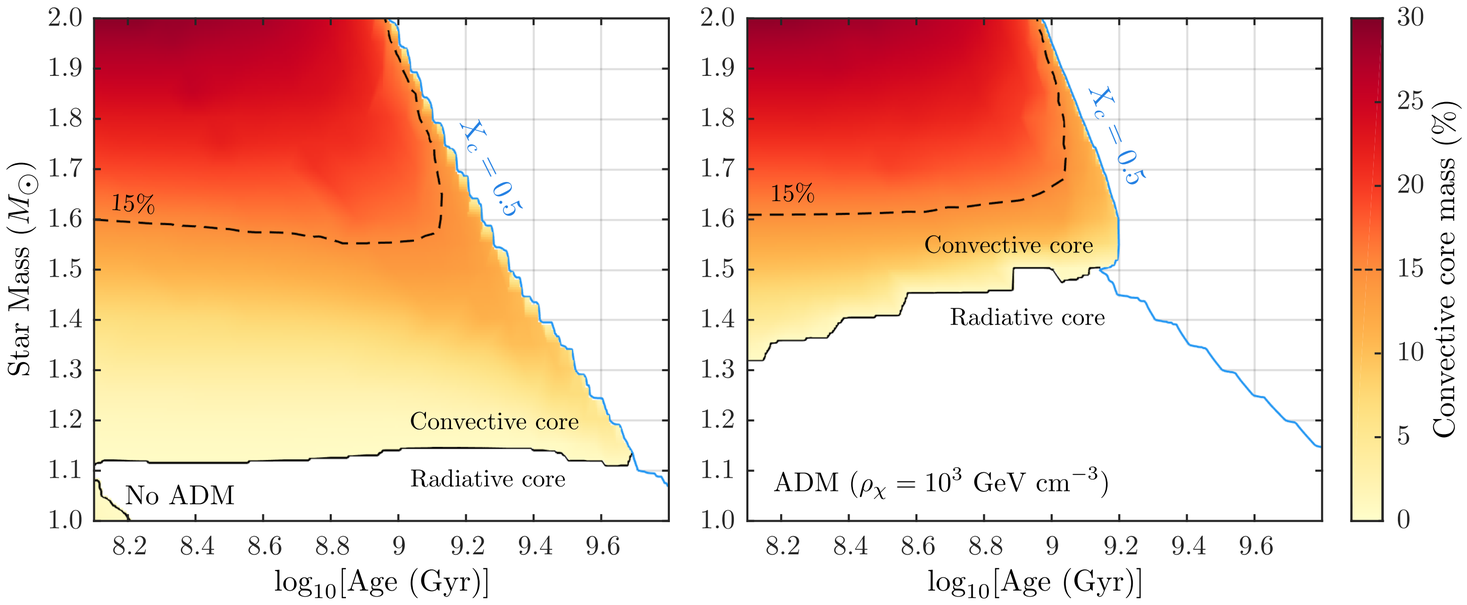

FIG. VII Mass of the convective core during the of MS of stars for with (right) and without (left) ADM. The blue line is represents the end of the MS. The black solid line separates stars with radiative core from stars with convective core.

Convective core suppression in the HR Diagram

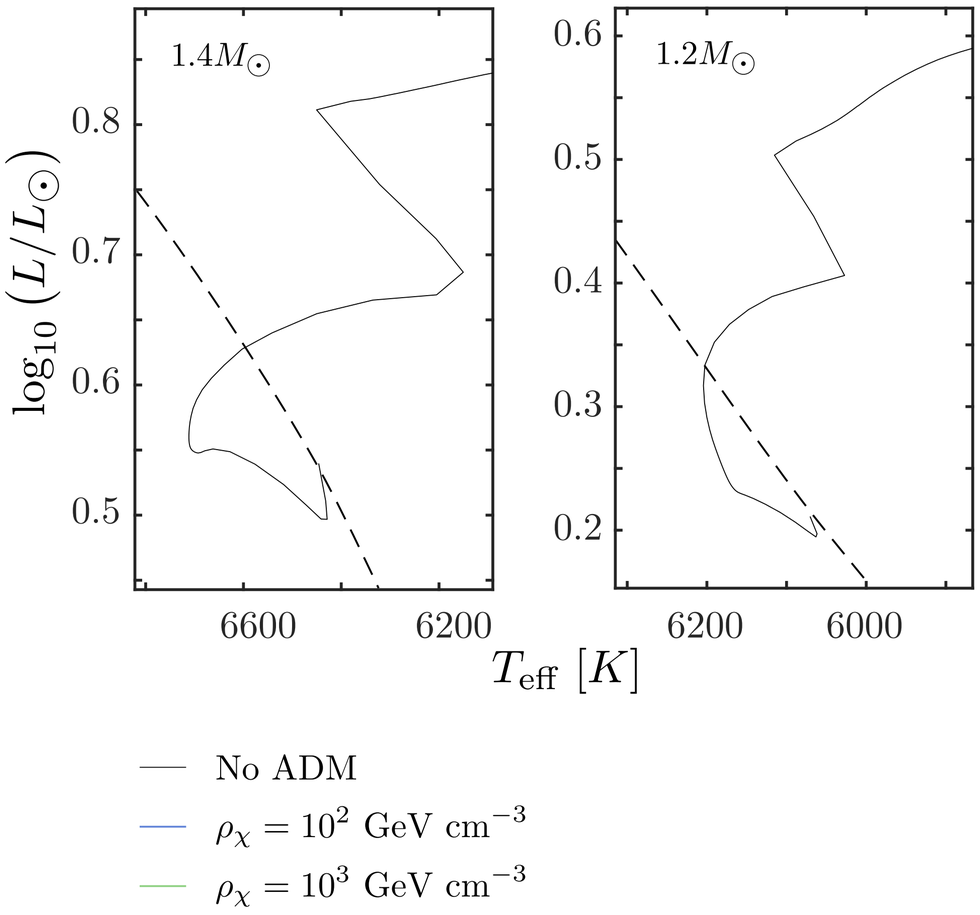

The standard abrupt stop of convection in MS stars is causes an abrupt change in the star´s effective temperature -> "**Main-sequence hook**".

If ADM energy transport is efficient and convection is avoided the hook feature is **suppressed**.

There is a **clear difference** in the evolutionary path of stars with M~1.4M⊙.

FIG. VIII Evolution of MS low-mass stars in the HR diagram, with and without ADM.

Convective core suppression in the HR Diagram

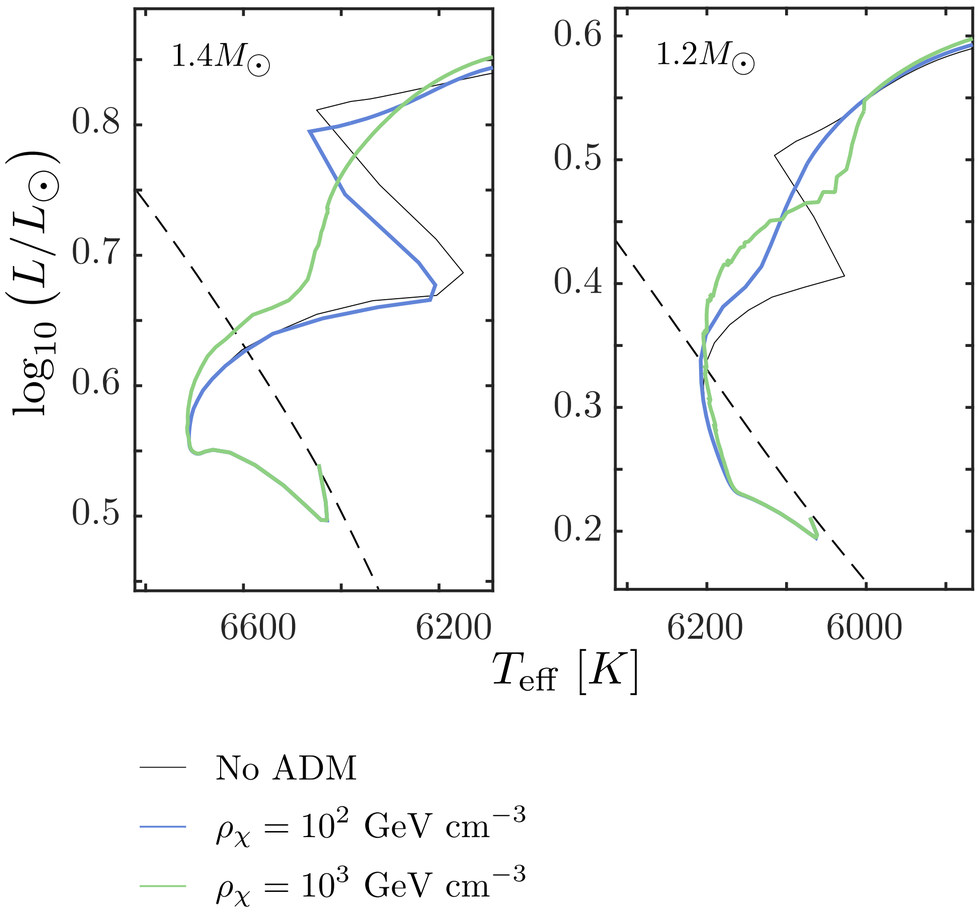

The standard abrupt stop of convection in MS stars is causes an abrupt change in the star´s effective temperature -> "**Main-sequence hook**".

If ADM energy transport is efficient and convection is avoided the hook feature is **suppressed**.

There is a **clear difference** in the evolutionary path of stars with M~1.4M⊙.

FIG. VIII Evolution of MS low-mass stars in the HR diagram, with and without ADM.

Dark matter impact in Isochrones

The **fit of isochrones** (curves with constant age) to the color magnitude diagram of stellar populations is the most used technique to date stars (e.g., **Soderlom 2010**).

Isochrones for ~ 2 Gyr are **sensible to the MS hook** of stars with M ~1.4M, which in turn are sensitive to the considered.

The absence of a discontinuity in the CMD of a stellar population with ~ 2 Gyr would be a **strong hint** to the suppression of core convection by ADM particles.

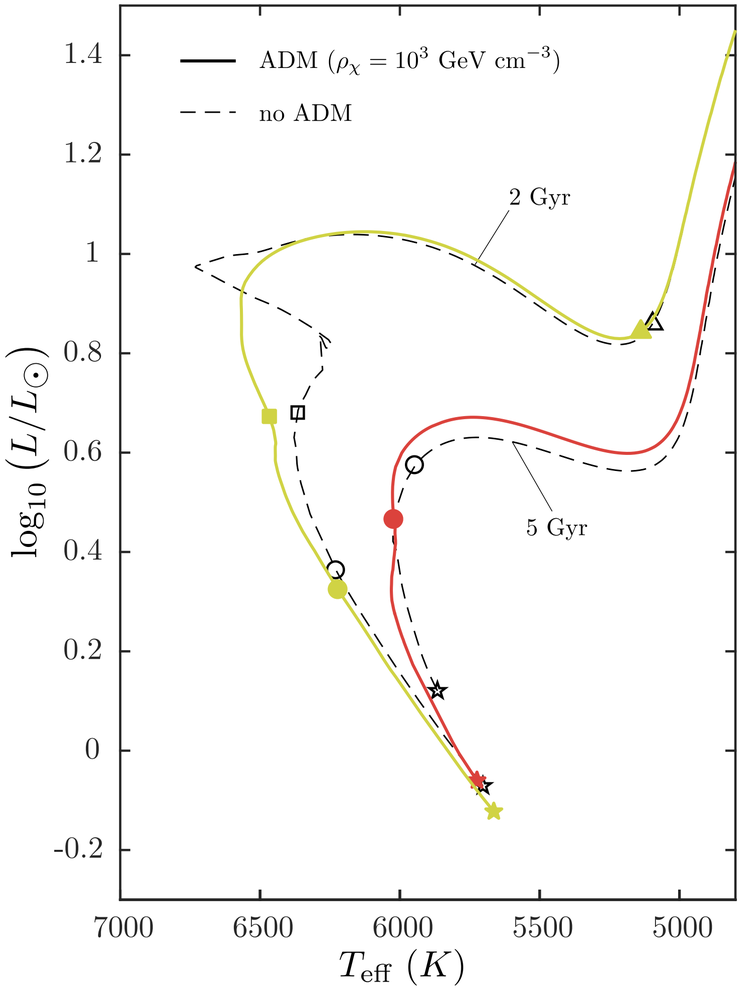

FIG. IX Isochrones for a simple stellar population in a scenario with (solid) and without (dashed) ADM. The markers along the isochrones, star, circle, square and triangle, represent stars with 1.0, 1.2, 1.4 and 1.6 $M_\odot$ respectively.

Dark matt

The **fit of isc**
magnitude c
technique to

Isochrones f
with M ~1.4M

The absence
population v
suppression

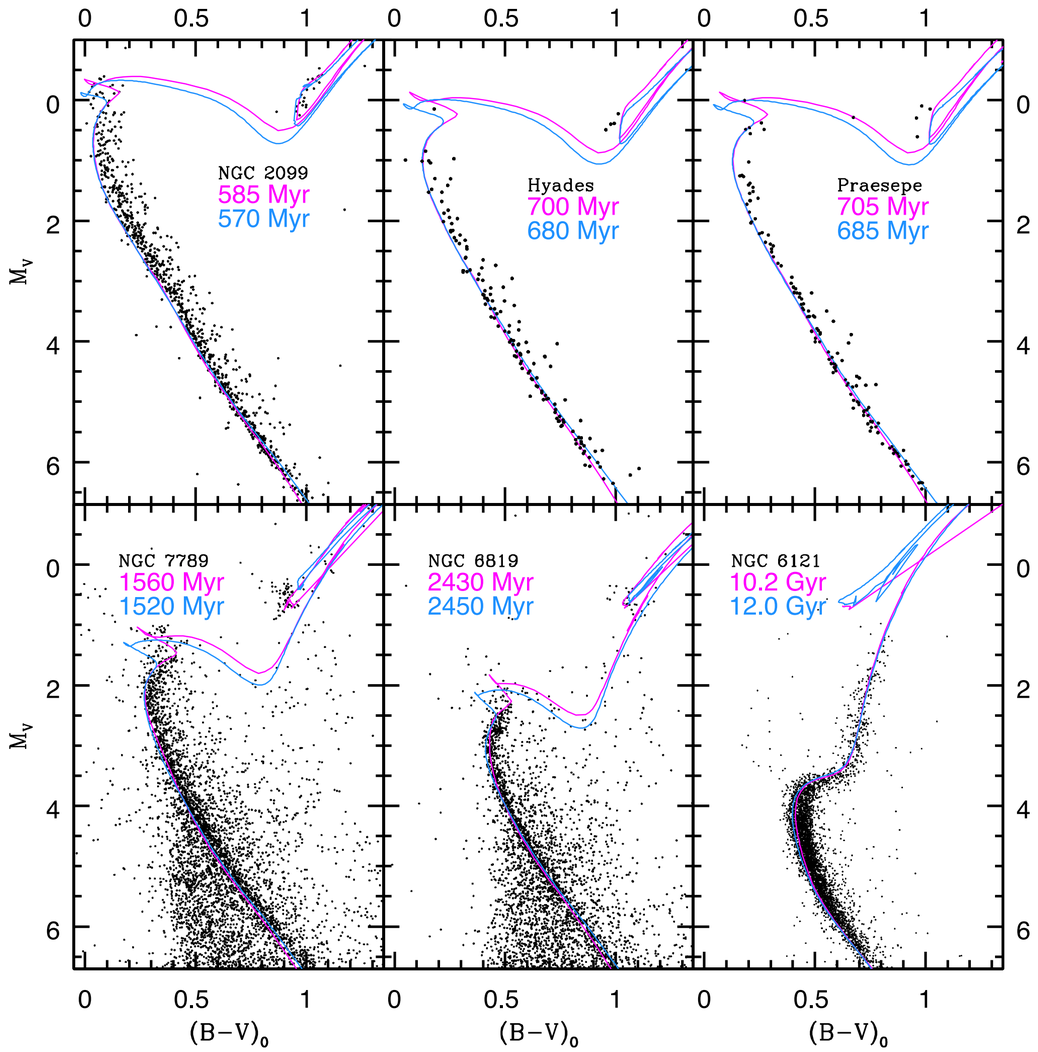

FIG. X Example of isochrones fitted to 6 star clusters. From **Cummings et al. 2018.**

FIG. IX Isochrones f
without (dashed) A
and triangle, repres

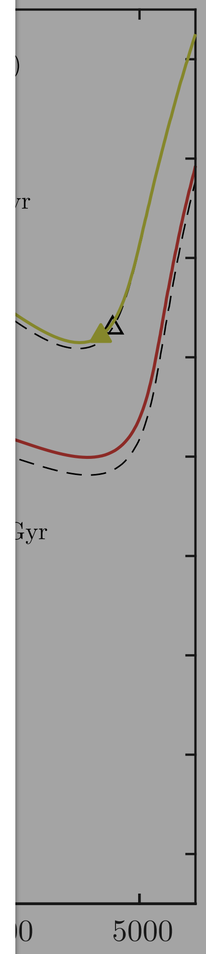

Dark matter impact in Isochrones

The **fit of isochrones** (curves with constant age) to the color magnitude diagram of stellar populations is the most used technique to date stars (e.g., **Soderlom 2010**).

Isochrones for ~ 2 Gyr are **sensible to the MS hook** of stars with M ~1.4M, which in turn are sensitive to the considered.

The absence of a discontinuity in the CMD of a stellar population with ~ 2 Gyr would be a **strong hint** to the suppression of core convection by ADM particles.

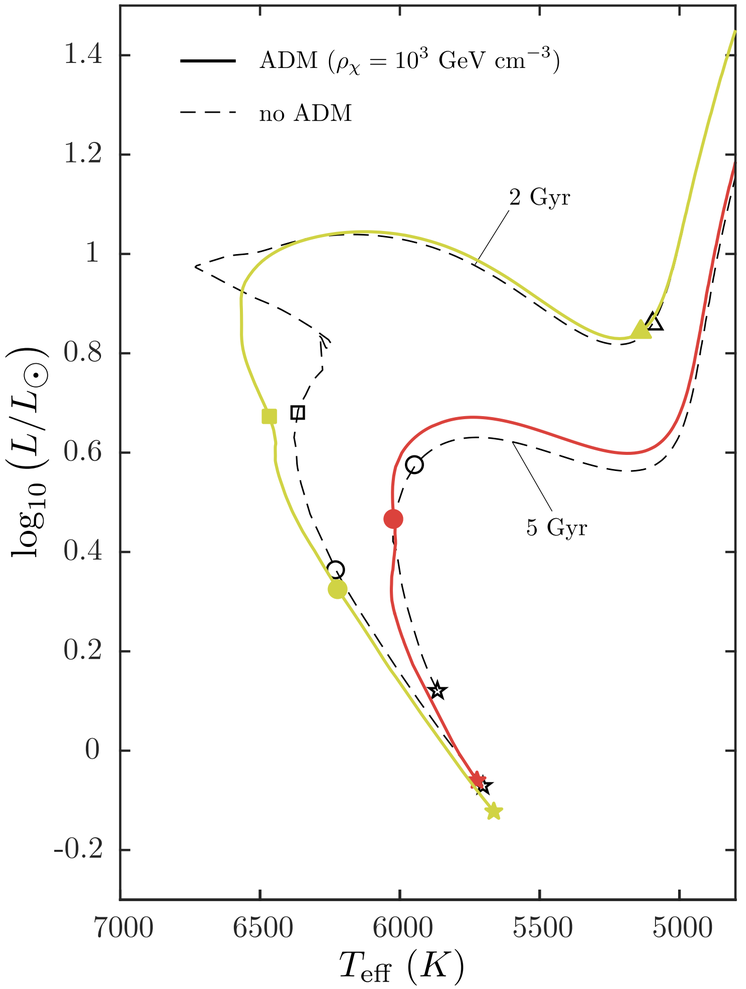

FIG. IX Isochrones for a simple stellar population in a scenario with (solid) and without (dashed) ADM. The markers along the isochrones, star, circle, square and triangle, represent stars with 1.0, 1.2, 1.4 and 1.6 $M_\odot$ respectively.

Introduction

Evidence to Particle Dark Matter

Stars as Dark Matter Laboratories

Energy transport by Particle Dark Matter

The code: dmEFT

Results

Asteroseismology of Red Clump Stars with Dark Matter

(**Lopes**, Lopes & Silk, *submitted*)

ADM in the Nuclear Star Cluster: Low Mass Main-Sequence Stars

(**Lopes** & Lopes, *ApJ, in press*)

Conclusion

Summary

Summary

We have developed dmEFT, the **first** code that computes dark matter (WIMP) phenomenology in the MESA (widely used in the community)

For the first time we showed that the **asteroseismology of Red Clump Stars** (abundant in asteroseismic surveys) can be used to **probe Dark Matter**.

Studied the implications of **ADM interactions** with baryons in the stellar population of thes **Nuclear Star Cluster.**

Studying other **interesting astrophysical scenarios** taking advantage of the full potential of dmEFT.

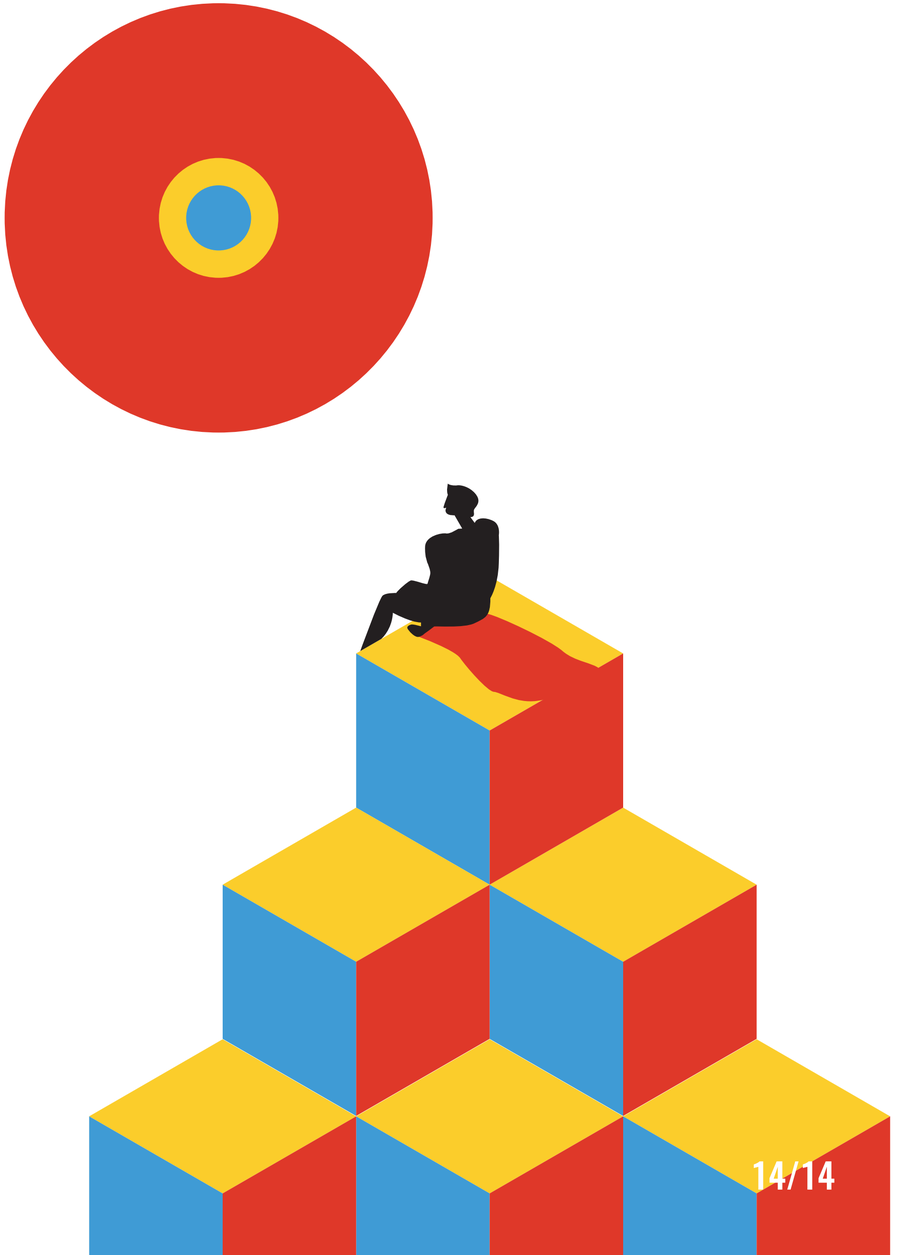

Zwicky, F. (1933), *Helvetica Physica Acta,* **Vol. 6, p. 110-127**

Rubin, V. C. & Ford, J., W. Kent (1970). *The Astrophysical Journal* **159, 379**.

Tucker, W., Blanco, P., Rappoport, S., et al. 1998, *Astrophysical Journal*, **496, L5**

Choi, K., Abe, K., Haga, Y., Hayato, Y., Iyogi, K., Kameda, J., et al. (2015). *Physical Review Letters*, **114(1), 141301.**

Lopes, I. P., & Silk, J. (2002). *Physical Review Letters*, **88(1), 151303**

Moskalenko, I. V. & Wai, L. (2007). *Astrophysical Journal*, **659(1), L29-L32**.

Paxton, B., Bildsten, L., Dotter, A., Herwig, F., Lesaffre, P., & Timmes, F. (2011). *The Astrophysical Journal Supplement*, **192(1), 3**

Paxton, B., Cantiello, M., Arras, P., Bildsten, L., Brown, E. F., Dotter, A., et al. (2013). *The Astrophysical Journal Supplement*, **208(1), 4**

Paxton, B., Marchant, P., Schwab, J., Bauer, E. B., Bildsten, L., Cantiello, M., et al. (2015). *The Astrophysical Journal Supplement Series*, **220(1), 15**.

Paxton, B., Schwab, J., Bauer, E. B., Bildsten, L., Blinnikov, S., Duffell, P., et al. (2018). *The Astrophysical Journal Supplement Series*, **234(2), 34**

Gould, A. (1987). *Astrophysical Journal*, **321, 571-585**

Girardi, L. (2016). *Annual Review of Astronomy and Astrophysics,* **54(1), 95-133**

Mosser, B., Benomar, O., Belkacem, K., Goupil, M. J., Lagarde, N., Michel, E., et al. (2014). *Astronomy & Astrophysics* , **572, L5**

Tassoul, M. (1980). *Astrophysical Journal Supplement Series*, **43, 469-490**

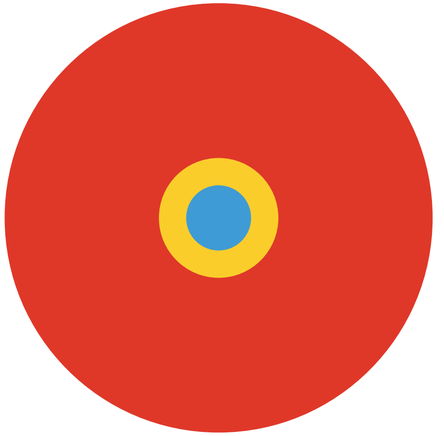

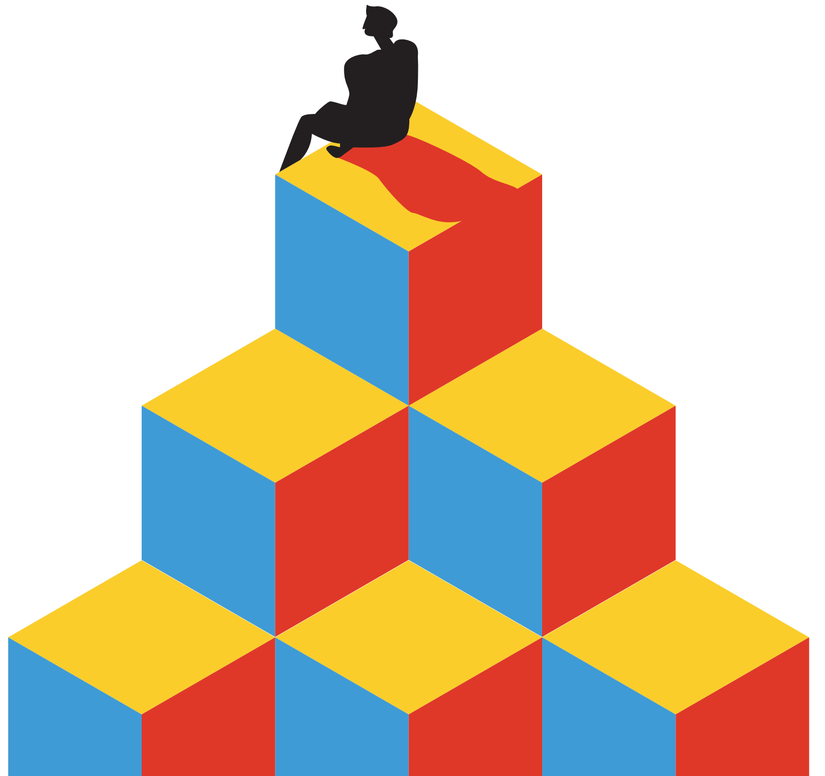

Montalban, J., Miglio, A., Noels, A., Dupret, M. A., Scuflaire, R., & Ventura, P. (2013). *The Astrophysical Journal*, **766(2), 118**

Genzel, R., Eisenhauer, F., & Gillessen, S. (2010). *Reviews of Modern Physics*, **82(4), 3121-3195**

Kaplan, D. E., Luty, M. A., & Zurek, K. M. (2009). *Physical Review D*, **79(1), 115016**

Soderblom, D. R. (2010). *Annual Review of Astronomy and Astrophysics*, **48(1), 581-629**

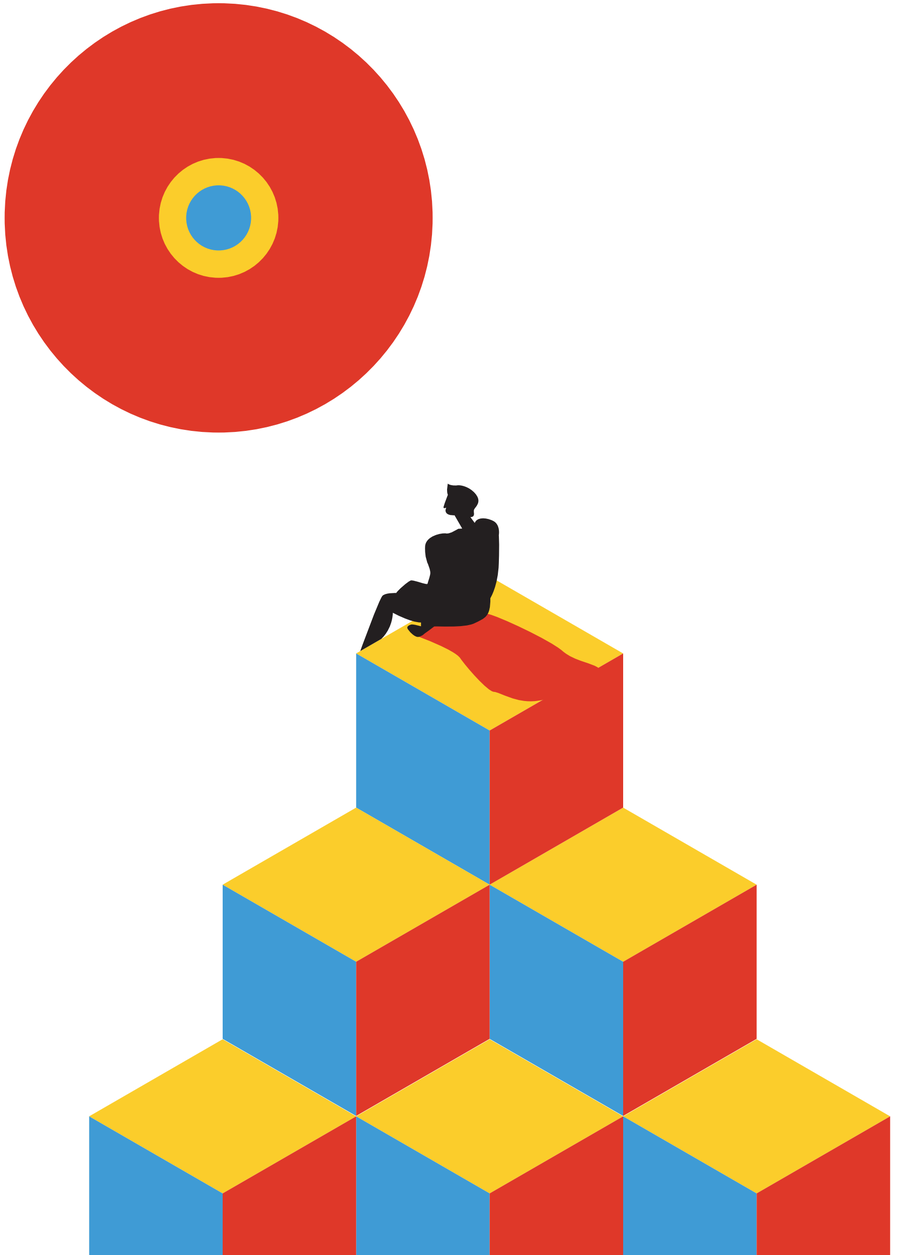

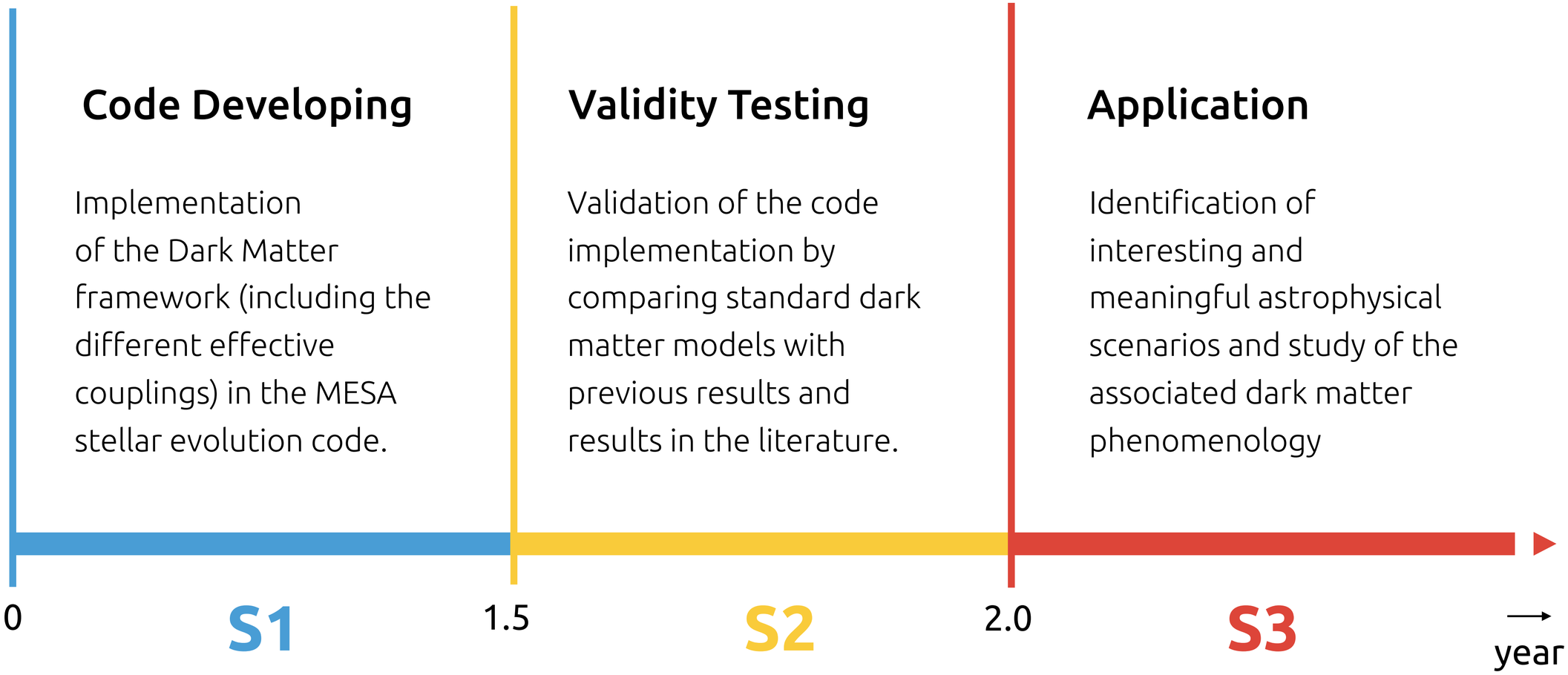
Code Developing
Implementation of the Dark Matter framework (including the different effective couplings) in the MESA stellar evolution code.
Validity Testing
Validation of the code implementation by comparing standard dark matter models with previous results and results in the literature.
Application
Identification of interesting and meaningful astrophysical scenarios and study of the associated dark matter phenomenology
0
S1
1.5
S2
2.0
S3
year

The different Physics of Stars

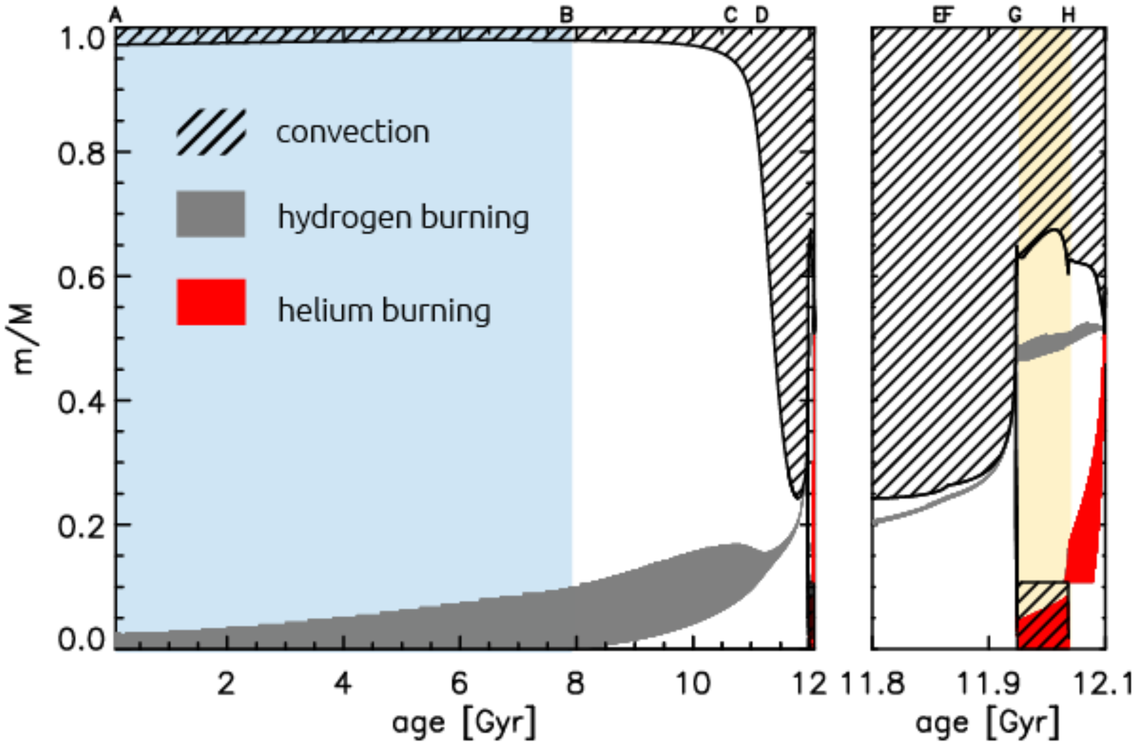

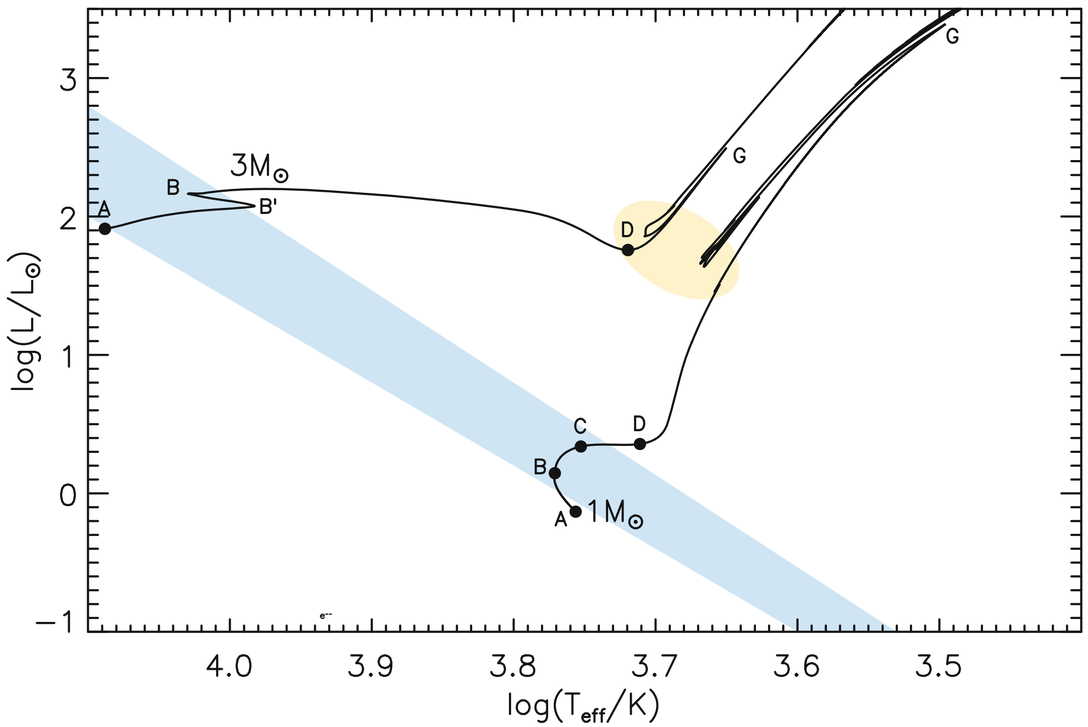

ANNEX I **Left:** Kippenhahn diagram for a 1 solar mass stars during the main-sequence (blue) through the Horizontal branch (yellow) up to the Asymptotic Giant Branch; **Right**: Evolution of two stars in the HR diagram. The color code is the same as the left figure. Letters mark important moments in the evolution of the star. Adapted from **Hekker & Dalsgaard (2017)**.

Dark Matter Constraints from experiments

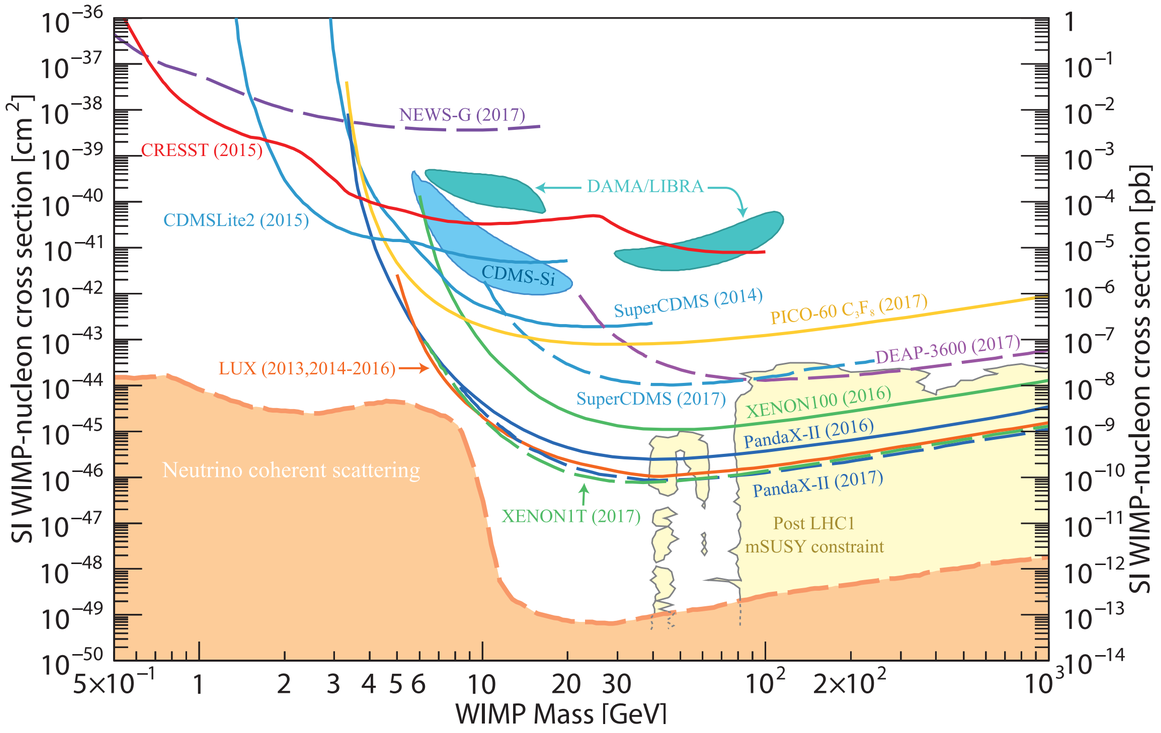

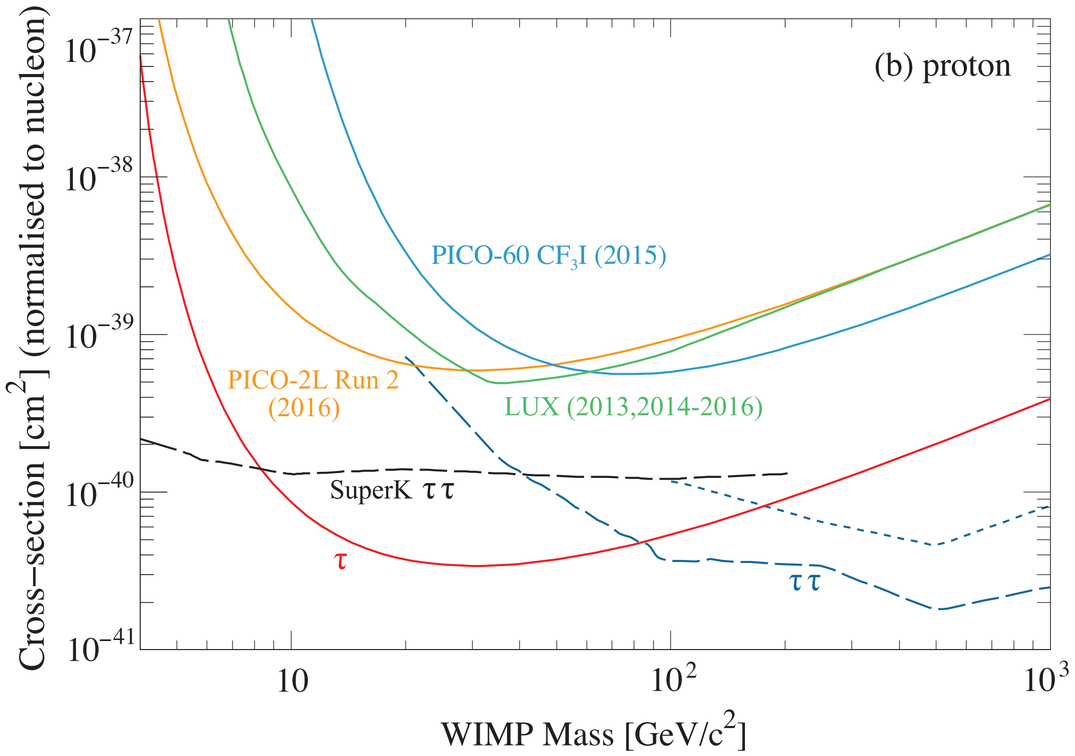

ANNEX II **Left:** Current constrains on the Dark Matter Spin Independent interaction cross-section ; **Right**: Current constrains on the Dark Matter Spin Dependent interaction cross-sectio (hydrogenn only). Adapted from **Tanabashi et al. (2018) (PDG)**.

Dark Matter Halo density Profile

Generalized ***Navarro-Frenk-White*** density profile:

$$\rho_{\mathrm{NFW}}(r) \simeq \frac{1}{\left(\frac{r}{r_s}\right)^{\gamma}\left[1+\frac{r}{r_s}\right]^{3-\gamma}} \qquad \text{(A1)}$$

Einasto density profile:

$$\rho_{\mathrm{Ein}}(r) \simeq e^{-\left(\frac{2}{a}\right)\left[\left(\frac{r}{r_s}\right)^{a}-1\right]} \qquad \text{(A2)}$$

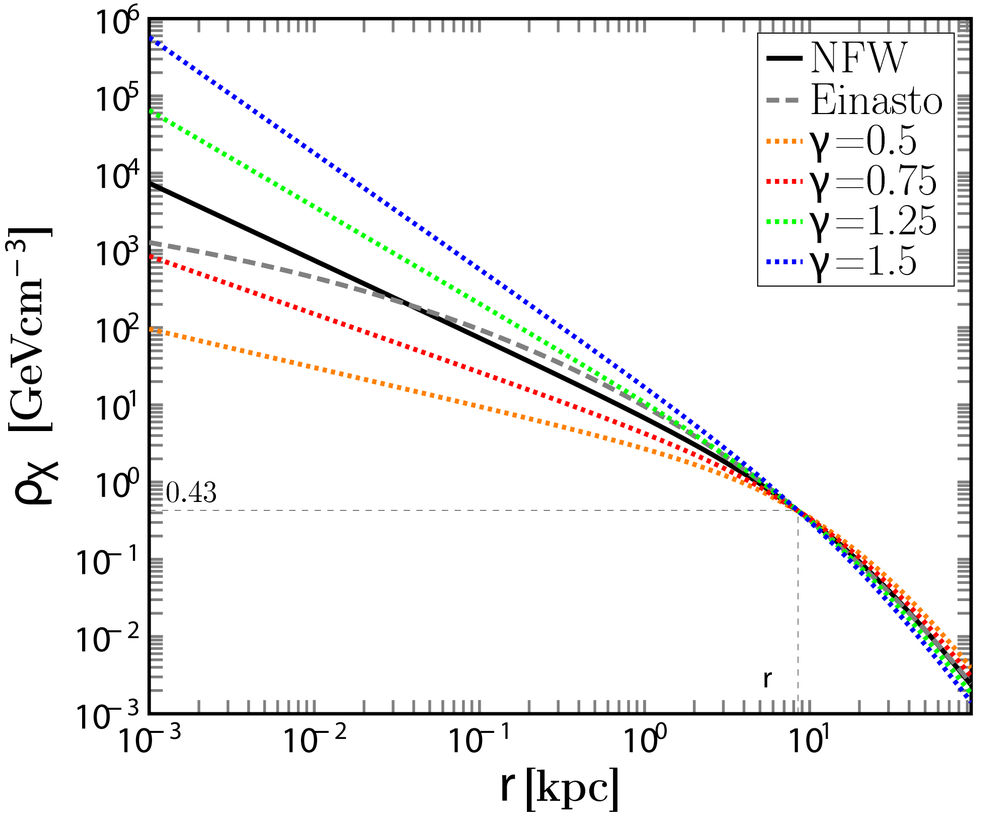

ANNEX III Dark Matter density halo profiles as a function of the distance to the center of the galaxy. Adapted from **Pierre et al. (2014).**

Dark Matter effective field theory

The **most general** non-relativistic elastic DM-Nucleon scattering can be described by the density Lagrangean

$$\mathcal{L}_{\rm int}(\vec{x}) = c\Psi^*_\chi(\vec{x})\mathcal{O}_\chi\Psi_\chi(\vec{x})\Psi^*_N(\vec{x})\mathcal{O}_N\Psi_N(\vec{x}) \qquad \text{(A4)}$$

$$\begin{aligned}
\hat{\mathcal{O}}_1 &= \mathbb{1}_{\chi N} & \hat{\mathcal{O}}_9 &= i\hat{\mathbf{S}}_\chi \cdot \left(\hat{\mathbf{S}}_N \times \frac{\hat{\mathbf{q}}}{m_N}\right) \\
\hat{\mathcal{O}}_3 &= i\hat{\mathbf{S}}_N \cdot \left(\frac{\hat{\mathbf{q}}}{m_N} \times \hat{\mathbf{v}}^\perp\right) & \hat{\mathcal{O}}_{10} &= i\hat{\mathbf{S}}_N \cdot \frac{\hat{\mathbf{q}}}{m_N} \\
\hat{\mathcal{O}}_4 &= \hat{\mathbf{S}}_\chi \cdot \hat{\mathbf{S}}_N & \hat{\mathcal{O}}_{11} &= i\hat{\mathbf{S}}_\chi \cdot \frac{\hat{\mathbf{q}}}{m_N} \\
\hat{\mathcal{O}}_5 &= i\hat{\mathbf{S}}_\chi \cdot \left(\frac{\hat{\mathbf{q}}}{m_N} \times \hat{\mathbf{v}}^\perp\right) & \hat{\mathcal{O}}_{12} &= \hat{\mathbf{S}}_\chi \cdot \left(\hat{\mathbf{S}}_N \times \hat{\mathbf{v}}^\perp\right) \\
\hat{\mathcal{O}}_6 &= \left(\hat{\mathbf{S}}_\chi \cdot \frac{\hat{\mathbf{q}}}{m_N}\right)\left(\hat{\mathbf{S}}_N \cdot \frac{\hat{\mathbf{q}}}{m_N}\right) & \hat{\mathcal{O}}_{13} &= i\left(\hat{\mathbf{S}}_\chi \cdot \hat{\mathbf{v}}^\perp\right)\left(\hat{\mathbf{S}}_N \cdot \frac{\hat{\mathbf{q}}}{m_N}\right) \\
\hat{\mathcal{O}}_7 &= \hat{\mathbf{S}}_N \cdot \hat{\mathbf{v}}^\perp & \hat{\mathcal{O}}_{14} &= i\left(\hat{\mathbf{S}}_\chi \cdot \frac{\hat{\mathbf{q}}}{m_N}\right)\left(\hat{\mathbf{S}}_N \cdot \hat{\mathbf{v}}^\perp\right) \\
\hat{\mathcal{O}}_8 &= \hat{\mathbf{S}}_\chi \cdot \hat{\mathbf{v}}^\perp & \hat{\mathcal{O}}_{15} &= -\left(\hat{\mathbf{S}}_\chi \cdot \frac{\hat{\mathbf{q}}}{m_N}\right)\left[\left(\hat{\mathbf{S}}_N \times \hat{\mathbf{v}}^\perp\right) \cdot \frac{\hat{\mathbf{q}}}{m_N}\right]
\end{aligned}$$

ANNEX IV Complete set of non-relativistic operators (at most linear in each of the 5 hermitian operators) allowed bay Galilean invariance and momentum conservation. Adapted from **Catena (2015)**.